Protease-Sensitive PEG Hydrogels Regulate Vascularization In Vitro and In Vivo

Marina Vigen, Jacob Ceccarelli, Andrew J. Putnam*

Forming functional blood vessel networks in engineered or ischemic tissues is a significant scientific and clinical hurdle. Poly(ethylene glycol) (PEG)-based hydrogels are adapted to investigate the role of mechanical properties and proteolytic susceptibility on vascularization. Four arm PEG vinyl sulfone is polymerized by Michael-type addition with cysteine groups on a slowly degraded matrix metalloprotease (MMP) susceptible peptide, GPQG↓IWGQ, or a more rapidly cleaved peptide, VPMS↓MRGG. Co-encapsulation of endothelial cells and supportive fibroblasts within the gels lead to vascular morphogenesis in vitro that is robust to changes in crosslinking peptide identity, but is significantly attenuated by increased crosslinking and MMP inhibition. Perfused vasculature forms from transplanted cells in vivo in all gel types; however, in contrast to the in vitro results, vascularization in vivo is not decreased in the more crosslinked gels. Collectively, these findings demonstrate the utility of this platform to support vascularization both in vitro and in vivo.

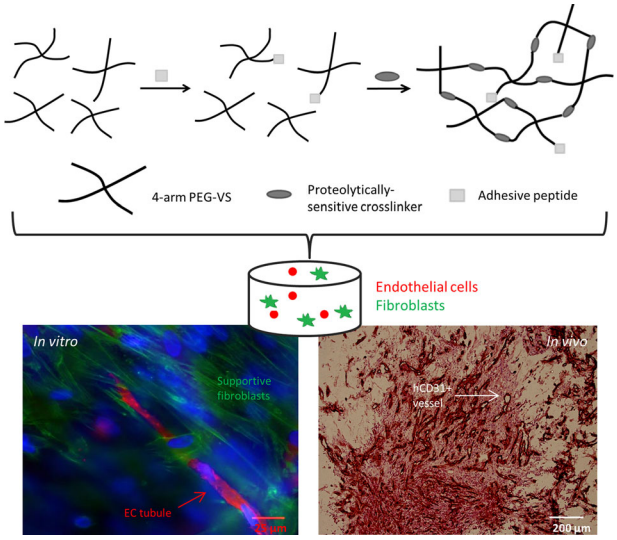

1. Introduction

Understanding and recapitulating angiogenesis in vitro and in vivo is of critical interest to the fields of tissue engineering and therapeutic angiogenesis. Current successes in tissue engineering are significantly limited by the inability to generate functional vasculature, which is necessary because diffusion is insufficient to meet the metabolic demands of larger tissues. Engineering vasculature is also of interest for the treatment of ischemic diseases, such as peripheral artery disease (PAD) and other related conditions.[1]

To address the need for vascularization, researchers have explored both cell and growth factor delivery from an appropriate scaffold.[2] In this work, we utilize an approach to therapeutic vascularization wherein endothelial cells (ECs) are delivered with supportive stromal cells in a biomaterial system that supports neovascularization in vivo.[3–5] Several studies have demonstrated the importance of stromal support in the formation of lumen-containing vessel structures in angiogenesis assays in vitro and in inosculation in vivo.[3,4,6–9] Natural hydrogel materials, such as fibrin, collagen, and Matrigel, have been widely used in this approach by our laboratory[3,9–12] and many others[5,13–17] because they are well known to support angiogenesis and vasculogenesis. However, such natural materials have many inherent limitations,

M. Vigen, Dr. J. Ceccarelli, Prof. A. J. Putnam
Department of Biomedical Engineering, University of Michigan, 2154 Lurie Biomedical Engineering Building, 1101 Beal Ave, Ann Arbor, MI 48109, USA
E-mail: putnam@umich.edu

DOI: 10.1002/mabi.201400161

including variability associated with the original source and processing approaches, the potential for immunogenicity, and undefined biological functionalities. Consequently, many investigators have pursued the use of synthetic materials with tailored biological functionalities as cell delivery vehicles.[18–21] Such materials offer the potential for enhanced control over cell function and allow investigation of the multiple roles of the extracellular matrix (ECM) on vascularization.

Peptide-functionalized poly(ethylene glycol) (PEG) hydrogel systems have been widely exploited to investigate the role of distinct biological signals in modulating cell invasion and in complex processes, such as vascularization, in vitro.[22–33] In these systems, PEG is typically functionalized with peptide sequences susceptible to cleavage by cell-derived matrix metalloproteases (MMPs) and with RGD, a minimal integrin-binding domain isolated from fibronectin that has been ubiquitously tethered to a variety of biomaterials to render them adhesive. The majority of early studies in this area utilized a MMP-cleavable peptide composed of a collagen-derived cleavage sequence, GPQG↓IWGQ (cleavage site indicated by ↓), with flanking regions on either side to facilitate crosslinking via thiol or amine chemistries. Cell invasion and vascularization were greatly improved in these gels as compared to non-degradable controls.[26,30,33] More recent studies have used more rapidly degraded MMP-cleavable peptides for in vitro studies of cell migration and vascularization with promising results.[25,29,34,35] Others have tuned mechanical properties of the construct to indirectly alter the extent of proteolysis needed to support robust vascularization.[29,30] As a whole, these prior studies suggest functionalized PEG gels are a viable option to support vascularization and warrant additional study.

Despite the wealth of studies elucidating the role of matrix mechanics and degradation in vasculogenesis in PEG hydrogels in vitro, the role of these properties in promoting vascularization in vivo is less clear. Instead, most efforts to date have focused primarily on utilizing PEG matrices for cell-demanded release of various factors.[36] Additionally, many of the materials utilized for promoting vascularization via growth factor delivery require fabrication ex vivo.[30,32,37–40] Though researchers have incorporated both GPQG↓IWGQ[30,32,37–39,41] and a more rapidly degraded peptide, VPMS↓MRGG,[35,42] into matrices utilized in vivo, variations in vascularization between these two variants has not been investigated directly. Several studies have demonstrated PEG hydrogels support the recruitment of host vasculature upon hydrogel delivery with growth factors[30,32,35,37–39,41] or growth factors with pancreatic islets[35,42] or MSCs.[40]

The goal of this work was to investigate the roles of gel mechanical properties and susceptibility to proteolysis in vascular morphogenesis in vitro and in vivo, and thereby bridge the gap between in vitro mechanistic studies and translation-focused in vivo applications. We fabricated PEG hydrogels via Michael-type addition of PEG macromers and cysteine-containing MMP-sensitive and adhesive peptides, and then characterized their ability to support vessel network formation from ECs and stromal fibroblasts. Two MMP-sensitive peptides were used for crosslinking, GPQG↓IWGQ (slow degradation) and VPMS↓MRGG (more rapid degradation). RGD was used as an adhesive moiety to facilitate cell attachment to the PEG gels. Materials were characterized and subsequently investigated for their capacity to support vascular morphogenesis over a period of two weeks in vitro and in subcutaneous pockets on the dorsal flank of SCID mice in vivo.

2. Experimental Section

2.1. Cell Isolation and Culture

Human umbilical vein endothelial cells (HUVECs, henceforth referred to as ECs) were isolated according to a previously established protocol.[43] ECs were cultured in supplemented endothelial growth medium (EGM-2, Lonza, Walkersville, MD) at 37 °C and 5% CO_2 and used at passage 3. Normal human lung fibroblasts (NHLFs, Lonza) were cultured in M199 (Invitrogen Corporation, Carlsbad, CA) with 10% fetal bovine serum (FBS), 1% penicillin/streptomycin (Mediatech, Manassas, VA), and 0.5% gentamicin (Invitrogen) at 37 °C and 5% CO_2 and used prior to passage 15. Cells were cultured in monolayers until reaching 80% confluency and passaged with 0.05% trypsin–EDTA (Invitrogen).

2.2. PEG Hydrogel Formation

Hydrogels were formed via a Michael-type addition reaction of 4-arm PEG vinyl sulfone (PEG-VS; 20 kDa, JenKem USA, Allen, TX) with a combination of thiol-containing adhesive and protease-sensitive peptides by modifying a published protocol.[44] To alter gel degradation rates, we selected two different peptides that are cleaved at different rates by several MMPs. In addition to proteolytic susceptibility, we altered gel solids content to investigate the role of initial mechanical properties on vascularization. To prepare the gels, PEG-VS was dissolved in HEPES (50 mM, pH 8.4, supplemented with growth factors from endothelial medium bullet kit) at the appropriate concentration to produce gels of 3.5 or 5% (w/v) total solids content. The adhesive peptide (CGRGDS, Genscript, Piscataway, NJ) was added to the PEG solution at 10 μg μL^{-1} in HEPES to yield a final adhesive site density upon gelation of 500 μM and the solution was reacted 30 min at room temperature. Following conjugation of RGD, bis-cysteine-containing crosslinking peptides were added in HEPES such that -SH and -VS groups were present at a 1:1 molar ratio. Gels were polymerized with one of two peptides, Ac-GCRD-GPQG↓IWGQ-DRCG-NH_2 or Ac-GCRD-VPMS↓MRGG-DRCG-NH_2 (Genscript, cleavage site indicated by ↓). Henceforth, gels polymerized with GPQG↓IWGQ and VPMS↓MRGG will be referred to as PEG-G and PEG-V gels, respectively. After mixing, precursor solutions (3.5% PEG-G, 5%

PEG-G, 3.5% PEG-V, and 5% PEG-V) were polymerized for 1 h at 37 °C in Teflon molds for rheology experiments or in sterile 1-ml syringes with the needle end cut off for all other experiments.[45] After polymerization, gels were transferred to medium or PBS, as appropriate. All gels were formed under aseptic conditions from precursors that were filtered through a 0.22 μm syringe filter.

2.3. Mechanical and Physical Characterization of PEG Gels

Bulk mechanical properties were characterized via parallel plate rheology on swollen gels. Following polymerization in Teflon molds, 100 μL gels were swollen overnight in PBS at 37 °C. Measurements were obtained on an AR G2 rheometer (TA Instruments, New Castle, DE) equipped with a Peltier stage and an 8 mm geometry. Both surfaces were coated with P800 sandpaper (3M, St. Paul, MN) and the gap was adjusted to apply a constant 0.1 N force to prevent slip during measurement. For each gel, a 5 min time sweep was followed by a frequency sweep from 0.1 to 10 Hz at 5% strain and then a strain sweep from 0.1 to 50% at 1 Hz. Reported shear storage modulus (G') values are the average over the linear viscoelastic region of the frequency sweep.

The equilibrium volumetric swelling ratio was also obtained for each gel type. Cell-free gels 50 μl in volume were polymerized in cut off syringes, as described above, and swollen at 37 °C in PBS for 48 h. At this point, each gel was weighed, frozen, and lyophilized, to give values for the wet and dry weight of each gel. The volumetric swelling ratio was calculated from the mass swelling ratio according to a previously described method:[46]

$$Q = 1 + \frac{\rho_{\text{polymer}}}{\rho_{\text{solvent}}}(q - 1) \quad (1)$$

where q is the mass swelling ratio (wet weight/final dry weight), ρ_{polymer} is the polymer density (1.07 g mL^{-1} for PEG), and ρ_{solvent} is the density of the buffer (1 g mL^{-1}).

Cell-mediated bulk hydrogel degradation was assessed by monitoring the swelling ratio of 50 μl gels containing 10^6 ECs mL^{-1} and 10^6 NHLFs mL^{-1}. Gels were cultured at 37 °C and 5% CO_2 up to 14 d. The swelling ratio was determined as for gels without cells.

2.4. Dextran Release from PEG Hydrogels

The bulk transport of dextran through the hydrogels was quantified as described previously[47] to probe the relative ease of diffusion of macromolecular species through different hydrogel formulations. Acellular hydrogels were prepared under aseptic conditions with 5 μg of 70 kDa Texas red-conjugated dextran (Life Technologies) incorporated in each 50 μl gel. Hydrogels were incubated in sterile PBS at 37 °C and the supernatant was aseptically collected and replaced with fresh PBS at 1, 3, 6, 12, 24, and 72 h after polymerization. After 72 h, gels were digested with 40 IU collagenase (Worthington Biochemical, Lakewood, NJ) in PBS to release any remaining dextran. The supernatants from each time point and the degraded gels were measured with a Fluoroskan Ascent FL (Thermo Scientific) plate reader at Ex:560/Em:620. The mass of dextran in each sample was determined by comparison to a standard curve of dextran in PBS.

2.5. Vasculogenesis Assay in PEG Hydrogels

ECs were fluorescently labeled via retroviral transduction with a gene encoding mCherry (Clonteck, Mountain View, CA) as previously described.[9] Lipofectamine 2000 (Life Technologies) was used to transfect Phoenix Ampho cells (Orbigen, San Diego, CA) with a plasmid encoding for mCherry. Viral supernatant was collected after 48 h, passed through a 0.45 μm syringe filter and supplemented with 5 μg mL^{-1} Polybrene (EMD Millipore, Billerica, MA) prior to incubation with EC for 6 h. The medium was changed to EGM-2 and cells were cultured overnight. Transduction was repeated via another round of viral infection the following day, and the ECs were then grown to confluence and used directly in the vasculogenesis assay. Constructs were polymerized in 50 μL aliquots using cut off syringes. Cell mixtures in a 1:1 ratio of ECs and NHLFs were added for a total of 10^5 cells/gel. Cell-seeded constructs were cultured in fully supplemented EGM-2 in a 12-well plate with the media changed every other day. At 7 and 14 d post-fabrication, gels from each condition were washed several times with PBS and then fixed with formalin prior to imaging. Low magnification fluorescent images were obtained of vessel network formation in each gel. Each gel was imaged at five locations in the interior of the gel using an Olympus IX81 spinning disk confocal microscope (Olympus, Center Valley, PA) with a Hammamatsu (Bridgewater, NJ) camera. Average total network length was determined as described previously[48] for each condition using the automated Angiogenesis Module in Metamorph Premier Software (Molecular Devices, Inc., Sunnyvale, CA).

To monitor the effect of inhibition of MMP or plasmin-mediated degradation on organization into vascular networks, a subset of experiments was conducted with GM6001 in dimethyl sulfoxide (DMSO) or aprotinin added to both the gel precursor solution and the culture medium. As a control, additional constructs were treated with the vehicle alone (DMSO). A broad-spectrum MMP inhibitor, GM6001 (EMD Chemicals, San Diego, CA), was added at 10 μM and the serine protease inhibitor aprotinin (Sigma) was added at 2.2 μM, as used in previous work from our lab.[10] Inhibitors were replenished with each media change. At 7 d post-fabrication, gels were fixed then imaged at low magnification.

2.6. PEG Hydrogel Implantation in SCID Mice and Laser Doppler Perfusion Imaging

All animal procedures were performed following a protocol approved by the University of Michigan Committee on Use and Care of Animals in accordance with NIH guidelines for the use of laboratory animals. Male six- to eight-week-old C.B.-17/SCID mice (Taconic Labs, Hudson, NY) were used for all experiments. Anesthetic/analgesic cocktail of 95 mg kg^{-1} ketamine (MWI Vet, Boise, ID), 9.5 mg kg^{-1} xylazine (MWI Vet), and 0.059 mg kg^{-1} buprenorphine (Bedford Laboratories, Bedford, OH) was delivered to each mouse via intraperitoneal injection. The dorsal flank of each mouse was cleared of fur by shaving followed by the application of a depilatory agent (Nair, Fisher Scientific, Pittsburgh, PA). The

region was then sterilized with betadine (Thermo Fisher Scientific, Fremont, CA) and wiped down with an alcohol pad. Implants ($n = 5$ per condition) were prepared as described above. Prior to initiation of the procedure, cell mixtures in a 1:1 ratio of ECs:NHLFs were prepared and aliquoted to yield a total of 3 million cells per injection sample (300 μl total volume, or 10 million total cells/ml). As prior studies from our lab using fibrin[49] and from others using PEG-VS gels without VEGF[37] have illustrated that minimal vascularization is seen in acellular controls, all implants contained cells and gel conditions alone were varied. Just prior to implantation, the bis-cysteine peptide in HEPES was combined with the PEG + RGD solution, the medium was aspirated from the top of the cell pellet, and the cells were resuspended in the gel precursor. Solutions were immediately injected subcutaneously on the dorsal flank of the mouse, with two implants placed per animal. Animals were kept stationary for 5 min to allow for implant gelation and then subjected to laser Doppler perfusion imaging (LDPI, Perimed AB, Sweden). Each mouse was imaged in triplicate. Mice were then placed in fresh cages for recovery. At Days 4, 7, and 14, mice were anesthetized with the cocktail described above and then subjected again to LDPI. Surgeons were not blinded to the experimental conditions.

2.7. Dextran Tracer Injection and Implant Removal

Implants were retrieved after 7 or 14 d following systemic administration of a 70 kDa Texas Red-conjugated dextran ($\lambda_{ex/em}$ of 595/615 nm, Invitrogen), used to assess inosculation of the transplanted cells within the implant with host vessels as described in previous work from our laboratory.[49] Following LDPI at each retrieval time point, each mouse was placed in a restraint device and 200 μL of a 5 mg mL^{-1} dextran solution in PBS was injected via the tail vein. After injection, mice were moved to fresh cages and the tracer was allowed to circulate systemically for 10 min. Animals were then euthanized and the implants were surgically excised.

2.8. Implant Processing and Histology

All explants were fixed 1 h in 4% PFA and then moved to 0.4% PFA overnight. Following fixation, samples were rinsed several times in cold PBS and then transferred to a sterile solution of 30% sucrose in PBS for 48 h at 4 °C. At this time, explants were transferred to a mixture containing two parts 30% sucrose in PBS and one part OCT embedding compound (Andwin Scientific, Schaumburg, IL) for another 24 h at 4 °C. Explants were then transferred to 100% OCT and kept another 24 h at 4 °C. Each sample was then finally embedded in 100% OCT in a disposable plastic mold (Fisher Scientific) and flash frozen on the surface of liquid nitrogen. Frozen sections were generated from each sample by the histology core at the University of Michigan School of Dentistry.

Sections were stained for human CD31 using both immunohistochemistry (IHC) and immunofluorescence (IF). After staining, sections were imaged using an Olympus IX81 spinning disk confocal microscope with a DP2-Twain (Olympus) color camera for visualizing IHC stained slides and a Hammamatsu camera for visualizing fluorescent-stained sections.

For IHC staining, tissues were warmed at room temperature and rinsed with PBS. Sections were incubated with 0.05% trypsin–EDTA for 10 min at 37 °C for antigen retrieval and washed with DI water then TBS-T. Sections were blocked 5 min using a peroxidase blocking solution (Dako EnVision System-HRP (DAB) kit, Dako, Carpinteria, CA). Primary antibody (human anti-mouse CD31, Dako) was diluted 1:50 in TBS-T and applied to slides. Following incubation overnight at 4 °C, slides were treated for 30 min with the HRP-conjugated anti-mouse secondary antibody provided in the kit. Prior to imaging, slides were mounted with xylene mounting medium (Fisher Scientific) and a #1 coverslip. One set of sections was imaged without any counterstain; the remaining sections were counterstained with hematoxylin and eosin and then imaged.

For IF staining, slides were warmed for 20 min then rinsed three times with PBS. Sections were blocked with 5% goat serum in PBS to eliminate non-specific protein binding. The primary antibody (human CD31; Santa Cruz Biotechnology, Inc., Santa Cruz, CA) was diluted 1:50 in 5% goat serum and added to samples for an overnight incubation at 4 °C. Following three washes with PBS, the secondary antibody (Alexa Fluor 488 goat anti-rabbit, Invitrogen) was added to tissues at a 1:100 dilution and tissues were incubated 30 min at room temperature. The unbound antibody was removed by three additional washes with PBS. Slides were then mounted with VectaShield (Vector Labs, Burlingame, CA) and covered with a #1 glass coverslip prior to imaging. Representative images were chosen for each condition.

Using sections stained with hCD31 via IHC, the number of blood vessels derived from transplanted human cells were quantified manually. Structures were considered blood vessels if they exhibited a rim of positive hCD31 stain and a hollow lumen. The average number of vessels per field of view in each section was determined by averaging the values obtained by two independent evaluators for at least five images per animal taken at 40 ×.

2.9. Statistics

All statistical analyses were performed using GraphPad Prism (GraphPad Software, La Jolla, CA). Data are from $n \geq 3$ and are reported as mean ± SEM. Analyses were performed with one or two-way ANOVA followed by Bonferroni's multiple comparison post-tests. Statistical significance was assumed when $p < 0.05$.

3. Results and Discussion

3.1. Gelation and Mechanical Characterization

PEG-based hydrogels were prepared by reacting PEG-VS with cysteine-containing adhesive peptides and bis-cysteine containing crosslinking peptides (see schematic in Figure 1A). Gelation occurred within 5 min and crosslinking was complete within 1 h, as assessed with shear rheology (data not shown). Mechanical characterization of pre-swollen gels composed of 3.5 and 5% w/v and each degradable peptide via shear rheology revealed that the storage modulus (G') did not vary as a function of the crosslinking

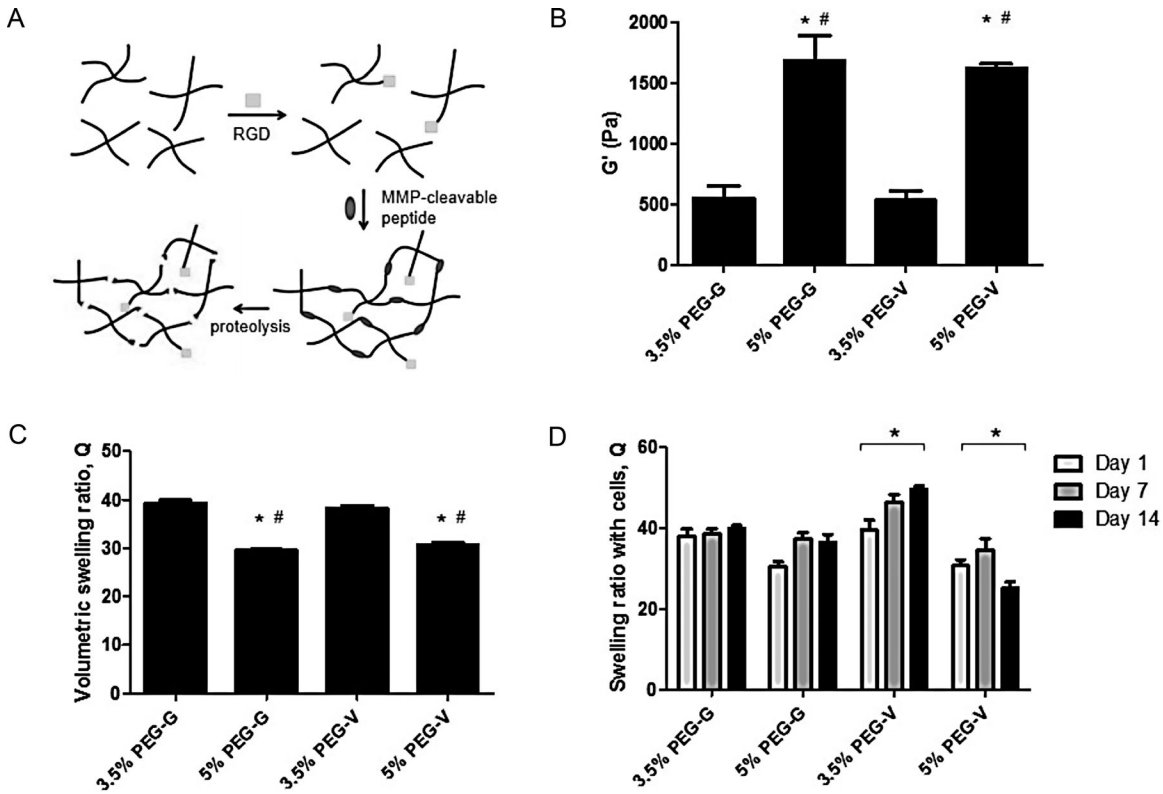

Figure 1. A) Hydrogels were formed via Michael type addition of cysteine containing RGD and MMP-degradable peptides (GCRD-GPQG↓IWGQ-DRCG and GCRD-VPMS↓MRGG-DRCG, cleavage at ↓) with 4-arm PEG vinyl sulfone. Gels are susceptible to MMP-mediated degradation but not hydrolysis. B) Hydrogels were polymerized, swollen, and their mechanical properties tested via shear rheology. All gels tested contain 500 μM RGD. *Significantly different from 3.5% G. #Significantly different from 3.5% V. $p < 0.05$, one-way ANOVA followed by Bonferroni post-tests. C) Volumetric swelling ratios of equilibrated acellular gels. *Significantly different from 3.5% G. #Significantly different from 3.5% V. $p < 0.05$, one-way ANOVA followed by Bonferroni post-tests. D) Swelling ratios of hydrogels containing cells changed significantly (indicated with *) from Day 1 to 14 in 3.5% and 5% V gels. $p < 0.05$, two-way ANOVA followed by Bonferroni post-tests.

peptide used, but increased significantly with increasing gel solids content (Figure 1B). Measurement of the volumetric swelling ratio for each gel type showed that the 3.5% gels swelled significantly more than 5% gels (Figure 1C). Extent of swelling did not significantly differ between PEG-G and PEG-V gels. As indicated by shear modulus and swelling ratio, changing solids content, but not peptide identity, significantly affected bulk network structure. These results corroborate the invariance of bulk mechanical properties to changing peptide identity demonstrated in another recent study.[50]

The swelling ratios of hydrogels containing cells were also obtained to characterize if cell-mediated remodeling of the gel networks varied as a function of crosslinking peptide identity (Figure 1D). At Day 1, swelling ratio values for each condition matched those obtained for gels without cells. Over 14 d, PEG-V gels with cells underwent significant changes in swelling behavior, which were not observed in PEG-G gels. These data suggest the encapsulated ECs and fibroblasts more rapidly degrade PEG-V than PEG-G gels, in agreement with the published comparative rates of degradation of the two peptides by MMPs 1 and 2.[25,51] However, since cells can both degrade the hydrogels and deposit new ECM proteins, changes in swelling ratio are only evidence of remodeling. Constructs without cells did not undergo significant changes in swelling over the course of 14 d (data not shown), implying proteolysis, and not hydrolysis mediates the observed effects.

3.2. Dextran Release from Hydrogels

Cumulative release profiles of fluorescent dextran were generated for each hydrogel, and the data were normalized to the total mass of dextran entrapped (Figure 2A). Experimental data were fit to the following equation, corresponding to a first-order exponential approximation[47] of Fickian diffusion through a planar slab,[52] using nonlinear least squares regression:

$$M = M_o + (M_f - M_o)[1 - e^{-Kt}] \quad (2)$$

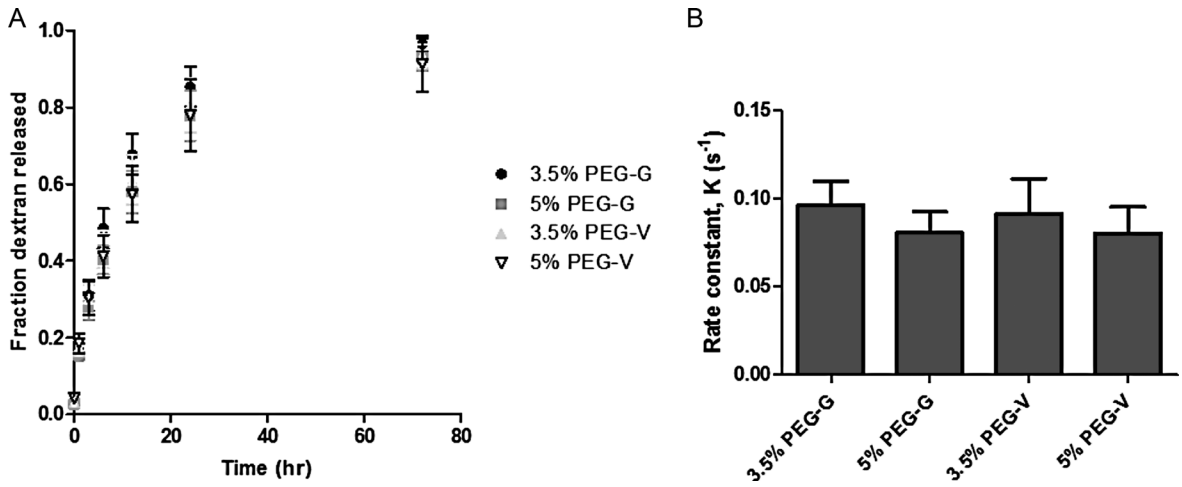

Figure 2. A) To assess bulk transport within the hydrogels, the release of 70 kDa Texas red-conjugated dextran entrapped within polymerized gels was measured over 72 h. B) Rate constants, *K*, were determined by fitting release profiles to a first-order exponential approximation. No significant differences were found across gel formulations. $p > 0.05$, sum-of-squares *F*-test.

The equation modeled the release data for 3.5% PEG-G, 5% PEG-G, 3.5% PEG-V, and 5% PEG-V gels (R^2: 0.91, 0.89, 0.80, and 0.85, respectively). From these data, the rate constant, *K*, was calculated for all hydrogel formulations, and a sum-of-squares *F*-test demonstrated no significant differences between release rates across gel formulation (Figure 2B). Thus, these data suggest the diffusive transport of large molecules does not vary significantly across the different gel formulations, despite differences in bulk mechanical properties.

3.3. Vascular Network Formation in PEG Gels In Vitro

Co-encapsulation of ECs and NHLFs in PEG-peptide hydrogels resulted in the formation of primitive capillary-like networks in all conditions over a period of two weeks (Figure 3A). The extent of vascularization, as measured by total network length, differed significantly based on gel identity (Figure 3B). Hydrogels with an initially high crosslink density (5 w/v% gels) supported vascular network formation, as measured by total network length, to a significantly lower degree over two weeks in culture than those gels with a lower initial crosslink density (3.5 w/v% gels) in PEG-G and PEG-V gels. This observed decrease is consistent with previous studies from our laboratory using PEG-collagen hydrogels,[47] and from another study that showed crosslinking density attenuated radial sprouting from endothelial and smooth muscle cell spheroids encapsulated in PEGDA-derived hydrogels.[29] Attenuated sprouting in the more crosslinked 5 w/v% gels was not attributed to changes in diffusive transport, as the diffusion of dextran tracers, as assessed above, was the same in all gel formulations. As a whole, these studies suggest initial hydrogel mechanical properties are an important modulator of vascular morphogenesis, even in matrices that cells can remodel.

The role of peptide identity on vascular network formation was also characterized (Figure 3). Network length at Day 7 was comparable between PEG-G and PEG-V gels at matching w/v%. By Day 14, PEG-V gels appeared qualitatively to support increased vessel network formation compared to Day 7 values and to PEG-G gels. However, the differences between Days 7 and 14 and between matched PEG-G and PEG-V gels were not statistically significant (Figure 3B), despite measured differences in swelling of PEG-G and PEG-V gels in the presence of cells that suggest the PEG-V gels are more rapidly remodeled. This may result from a delay between the onset of degradation and matrix vascularization, an idea corroborated by the qualitative increase in vascularization of PEG-V versus PEG-G gels at Day 14. Alternately, the increased swelling of PEG-V gels in the presence of cells may be a direct consequence of the fibroblasts rather than the ECs, and thus may not be a good proxy for assessing local matrix degradation around the sprouting tubules.

Vascular network formation within these hydrogels was also verified to be MMP-dependent based on the observation that morphogenesis was attenuated in the presence of the broad-spectrum MMP inhibitor, GM6001 (Figure 4). ECs remained round and did not organize into tubules in the presence of GM6001 in all gel formulations tested, regardless of peptide identity or hydrogel w/v%. By contrast, the addition of either a DMSO vehicle or the serine protease inhibitor aprotinin had no significant effects. Fibroblast migration in similar gels has also been

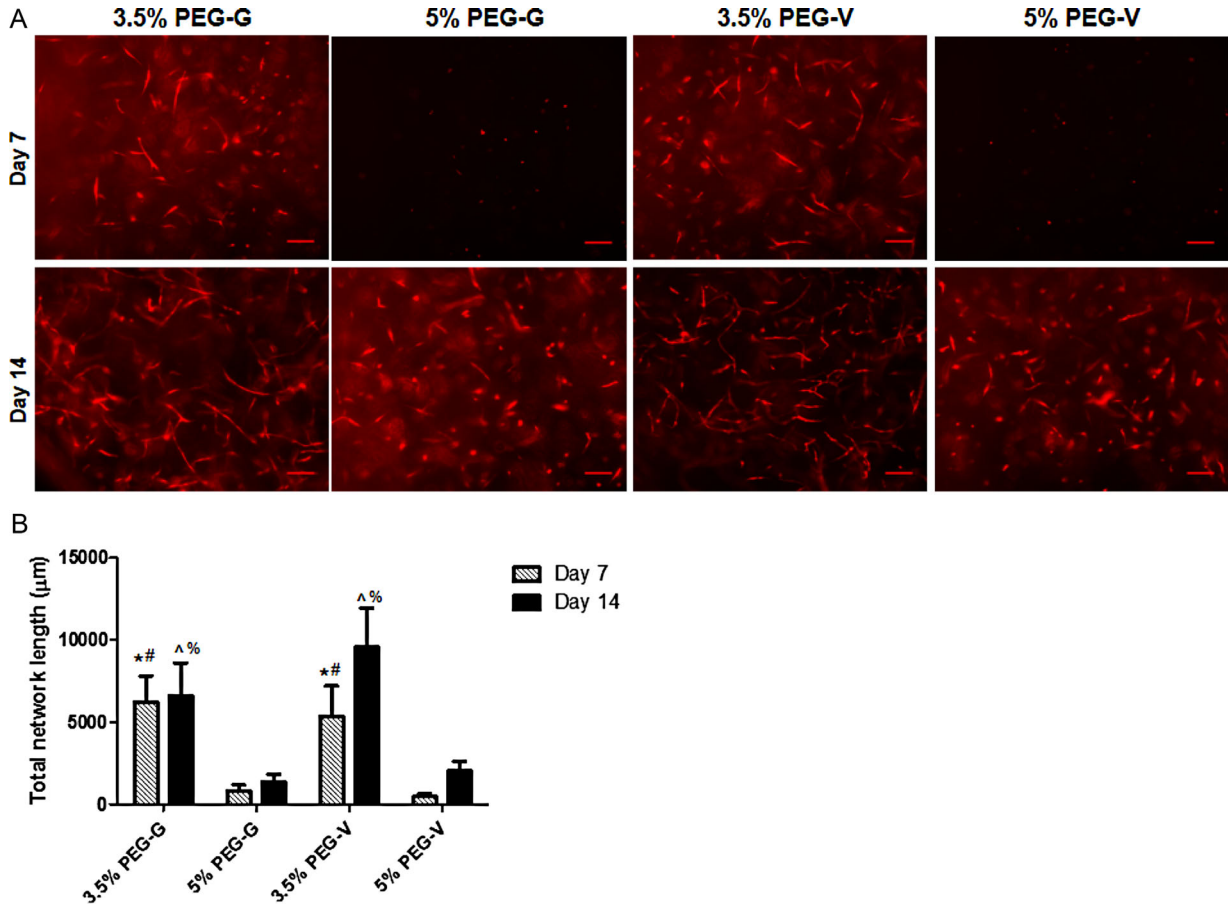

Figure 3. Vasculogenesis in vitro was monitored in PEG hydrogels of different w/v% and cross-linked with either of two degradable peptides. A) mCherry tagged ECs co-encapsulated with unlabeled fibroblasts organized into vascular networks in gels, and were imaged after 7 or 14 d (scale bars = 200 μm). B) Quantification of the total lengths of the vessel networks showed that the extent of vascularization was significantly higher in lower w/v% gels and slightly increased at later time points in PEG-V gels. Significant differences were found via one-way ANOVA followed by Bonferroni post-tests and are indicated according to the following symbols: ⋆compared to 5% PEG-G at 7 d, #compared to 5% PEG-V at 7 d, ^compared to 5% PEG-G at 14 d, and % compared to 5% PEG-V at 14 d, $p < 0.05$.

shown to depend on MMPs,[26,53] but these data demonstrate that MMPs are also required for vascularization in these gels.

3.4. Non-Invasive Perfusion Measurement of PEG Hydrogels Implanted In Vivo

PEG hydrogels containing ECs and NHLFs were injected subcutaneously on the dorsal flank of SCID mice and the vascularization by the implanted cells and subsequent inosculation with the host were monitored over 14 d. LDPI was used to monitor perfusion through the implant non-invasively (Figure 5). For all conditions, perfusion qualitatively increased over the course of the experiment. LDPI data suggest the rate of implant perfusion differs as a function of peptide identity, with significant increases in perfusion seen between 0 and 4 d for PEG-V gels only. In contrast, PEG-G gels appear to undergo less pronounced and slower changes in perfusion, particularly between 0 and 4 d, as assessed by LDPI.

3.5. Histological Analysis of Harvested Tissues

Vessels formed from transplanted human cells in all PEG constructs, and the resulting vessels were shown to inosculate with the host vasculature within 7 d after delivery of the cells within the gels. Upon retrieval from the subcutaneous space, the implanted PEG-based constructs exhibited visible redness (Figure 6). Cryosections stained for human CD31 and H&E demonstrated that all four of the hydrogel compositions tested supported the transplanted human ECs (Figure 7A). These human CD31-stained sections showed the presence of lumen-containing networks (arrows) containing host erythrocytes, indicating the

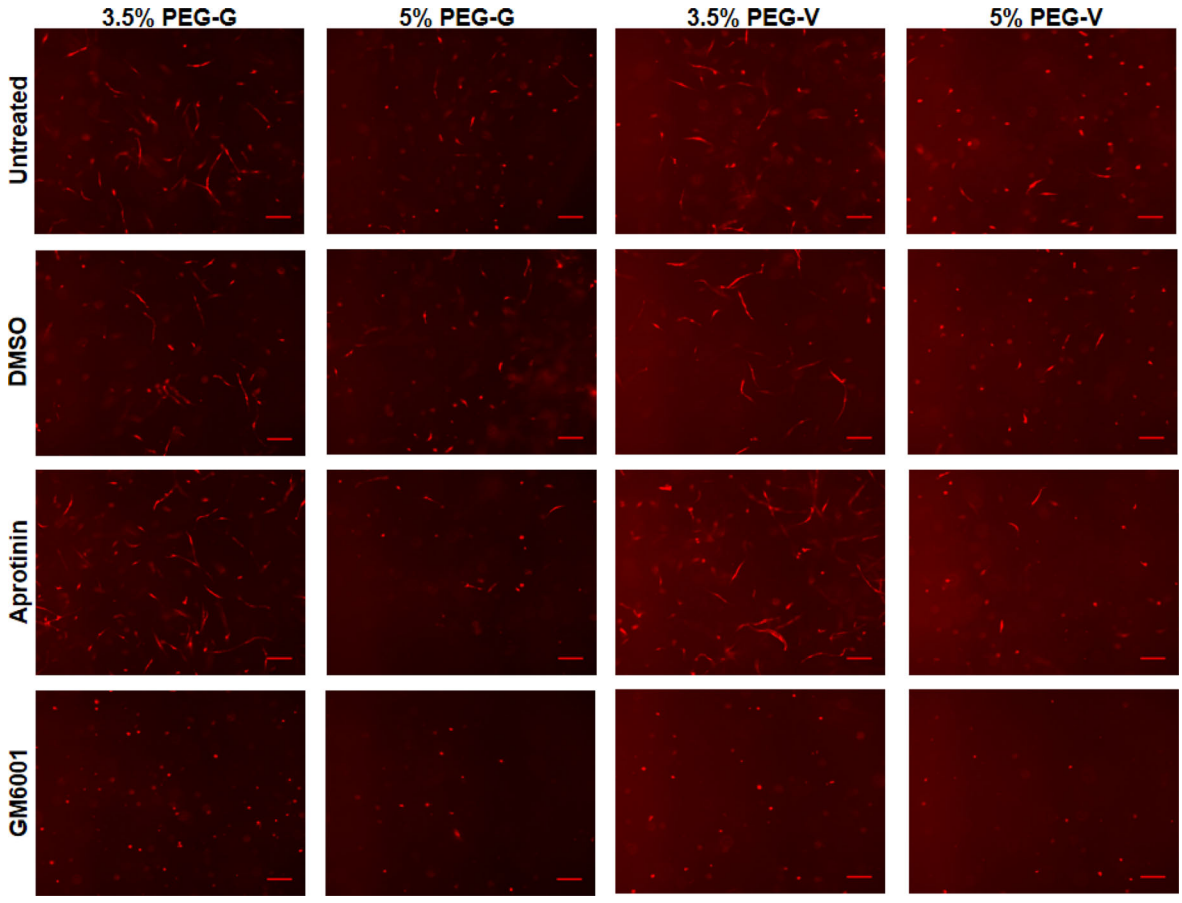

Figure 4. Vasculogenesis was monitored in vitro in gels of different w/v% and crosslinking peptides in untreated control gels and in the presence of 10 μM GM6001, DMSO, or 2.2 μM aprotinin in gels and culture media. mCherry tagged-ECs co-encapsulated with unlabeled fibroblasts organized into vascular networks in control gels and in gels containing DMSO or aprotinin, but not in gels containing GM6001. Constructs were fixed and imaged after 7 d (scale bars = 200 μm).

formation of a perfused vascular network from the transplanted human ECs for all gel formulations tested (Figure 7A). Systemic administration of a fluorescent dextran tracer further confirmed inosculation of host vessels with the neovessels of human cell origin that form within the PEG gels. Imaging of cryosectioned implants stained with hCD31 from tracer-injected animals revealed dextran-perfused vessels (red) lined with human CD31+ cells (green) in all gel types (Figure 8). All implants contained a clearly delineated border between mouse tissue and the PEG gel, suggesting that the ingrowth of host connective tissue into these PEG gels is relatively slow. Local gel degradation and cell-mediated matrix deposition in the periphery of vessels, illustrated by the presence of eosinophilic matrix around hCD31-stained vasculature, were observed.

Qualitatively, differences in vasculature were observed across conditions. However, quantification of vessel density showed the extent of vascularization differed significantly only between 3.5 and 5% PEG-V implants harvested at 7 d (Figure 7B). The increase in vascularization at Day 7 for 5% PEG-V gels was unexpected given the results of the in vitro studies. This difference may be due to differences in levels of protease activity and in protease identity in the two scenarios. In vivo, proteases are secreted by a variety of cell types, including interstitial and inflammatory cells in addition to ECs.[54] Our in vitro model only accounts for the contribution of endothelial and stromal support cells. Thus, matrices may be remodeled more rapidly in vivo, which may alter the initial mechanical environment that supports vascularization. As others have suggested previously in the context of cell migration,[26] excessive degradation of less crosslinked matrices may impair the ability of cells to generate traction upon matrix cleavage. These data demonstrate that the set of matrix cues determined to be optimal for vascular morphogenesis in vitro may not be the same ones necessary to maximize vascularization in vivo, and motivate further investigation of these materials in vivo.

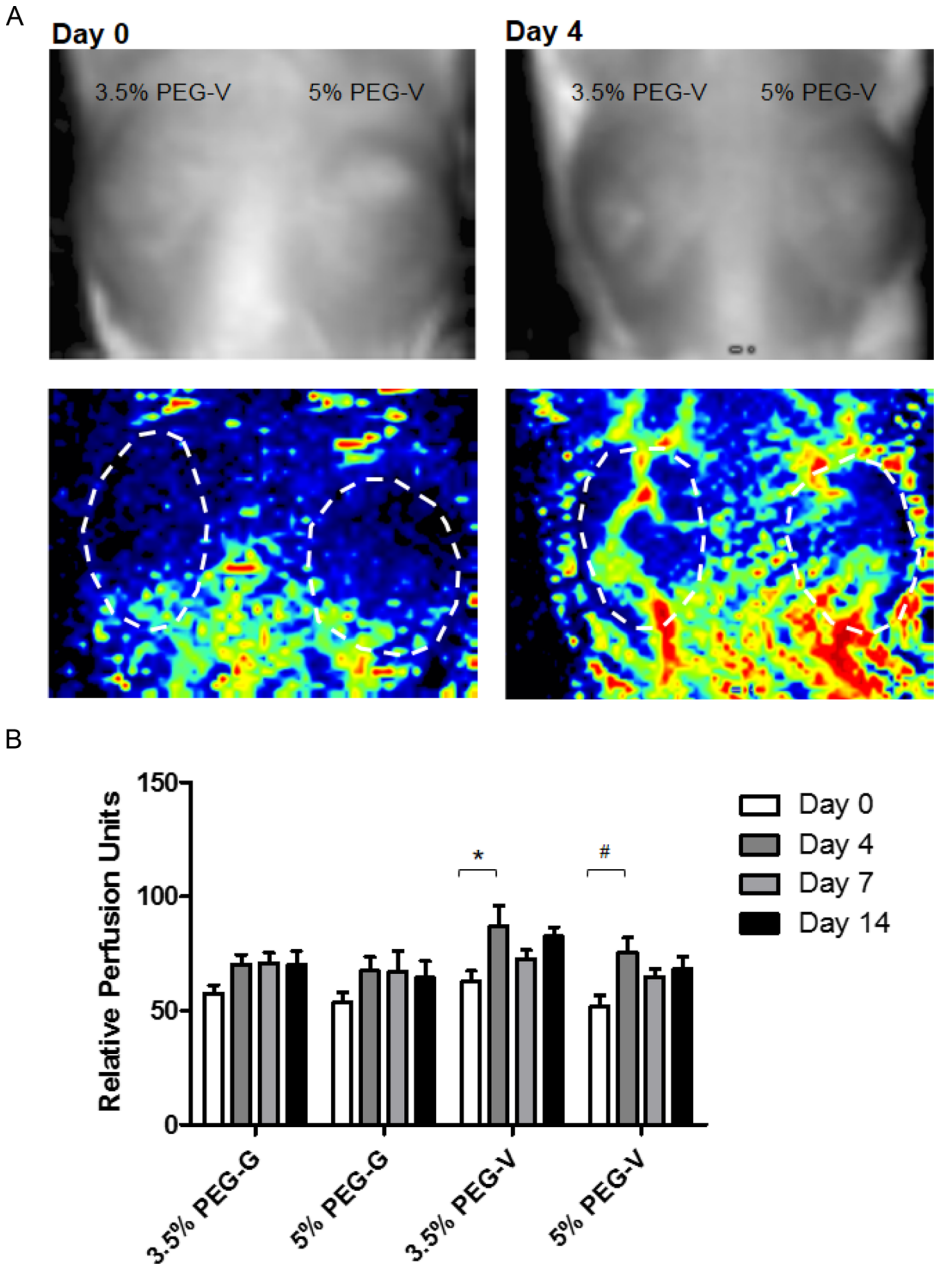

Figure 5. Laser Doppler perfusion imaging was used to non-invasively quantify blood flow after subcutaneous injection of gel constructs. A) Upper images show implant location on mouse. Lower images are LDPI heat maps indicating degree of perfusion. B) Quantification of relative perfusion shows differences between gel constructs. Statistically significant effects for both day and gel composition were found by two-way ANOVA. Statistically significant increases in perfusion were observed from Days 0 to 4 for 3.5% PEG-V (*) and 5% PEG-V (#). $p < 0.05$ two-way ANOVA followed by Bonferroni post-tests.

4. Conclusion

In this study, we demonstrated PEG hydrogels functionalized with adhesive and MMP-degradable peptides support the formation of vascular networks from encapsulated cells both in vitro and in vivo. By varying the solids content of the hydrogels and the identity of the protease-sensitive crosslinking peptides, we investigated the respective roles of gel mechanical properties and the kinetics of proteolysis on network formation. Our in vitro results showed that increasing solids content to increase gel mechanical properties significantly attenuated vascular morphogenesis in 3D, but that the formation of vessel networks was quantitatively similar for the two different crosslinking

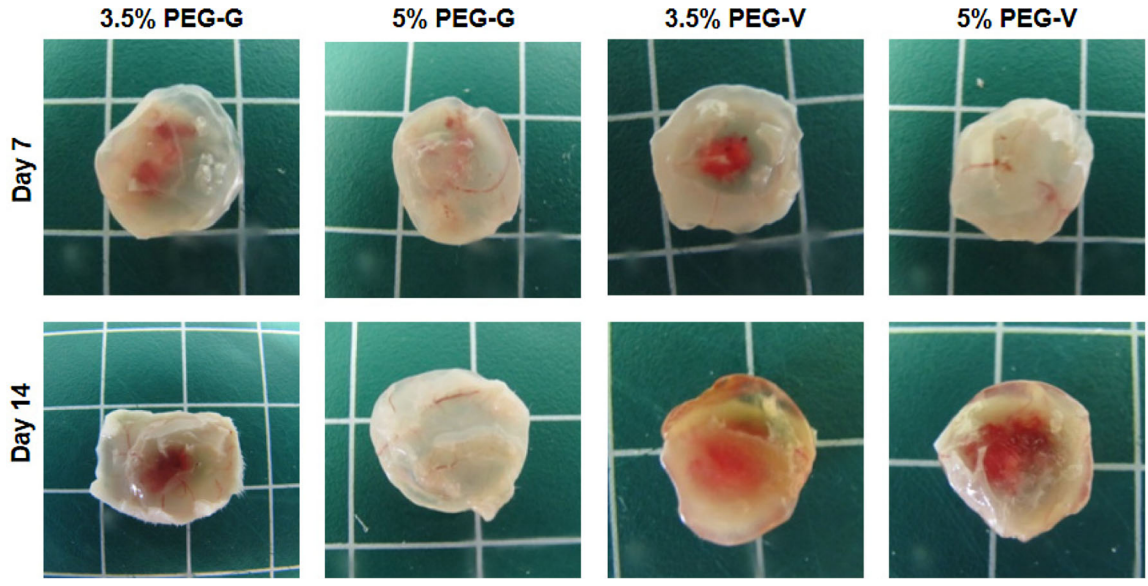

Figure 6. Macroscopic images of implants harvested at Days 7 and 14. Visible redness within implants suggested implant vasculature inosculated with host vessels in all gel constructs after implantation.

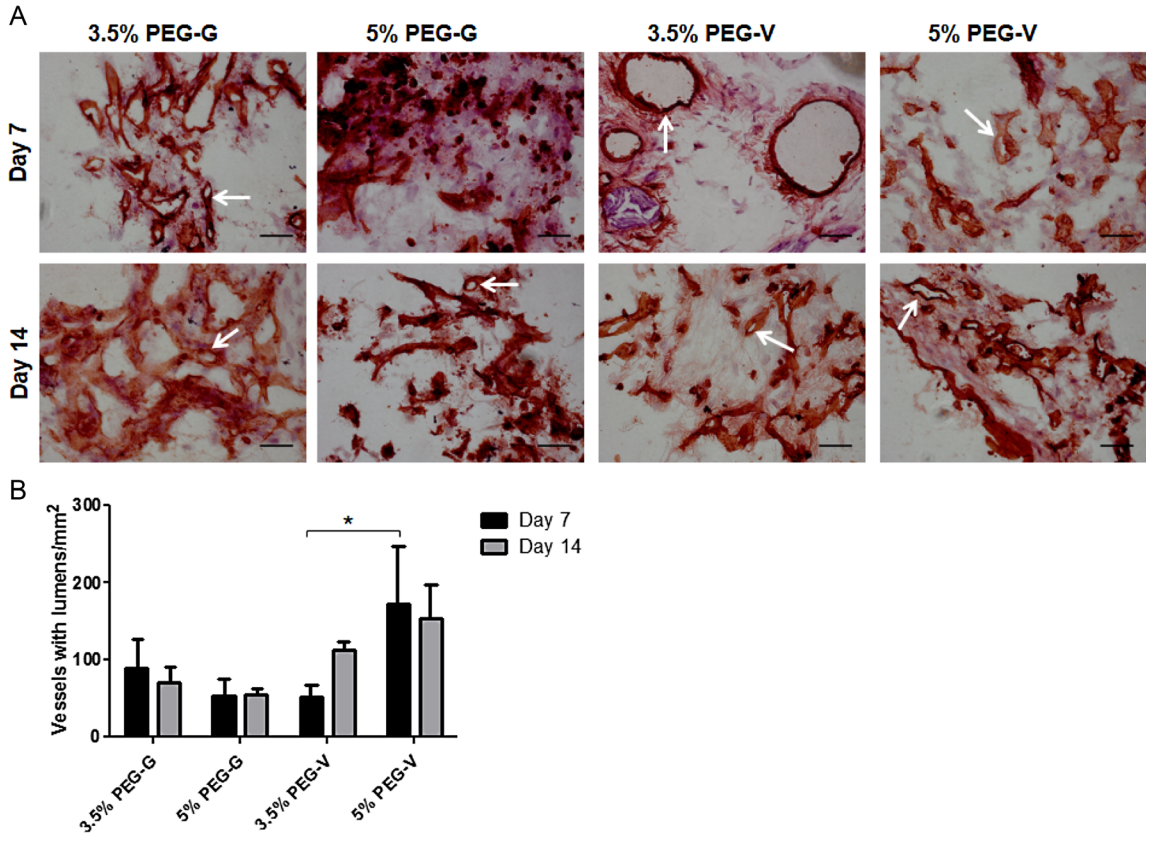

Figure 7. A) IHC and H&E staining of cryosections from implants retrieved after 7 or 14 d in vivo. Sections were stained for human CD31, counterstained with H&E, and then imaged at 40× (scale bars = 50 μm). Arrows point to representative hCD31-positive vessels. B) Vessel density was quantified from stained sections and compared with a two-way ANOVA followed by Bonferroni post-tests. There was a significantly higher density of vessels in the 5% PEG-V gels compared to the 3.5% PEG-V gels at 7 d.

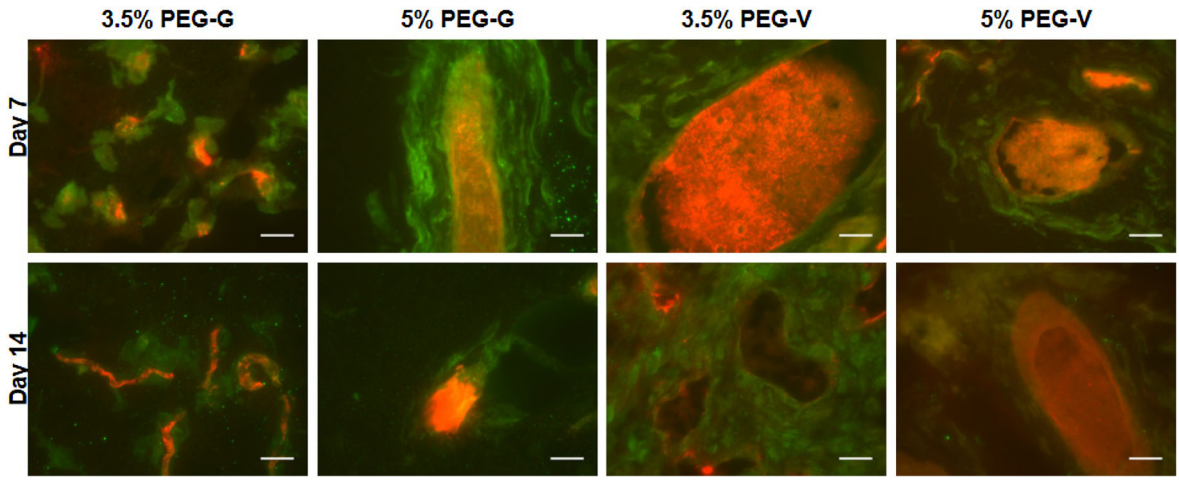

Figure 8. Red fluorescent 70-kDa dextran was administered systemically to mice prior to implant retrieval on Day 7. Following fixation and cryosectioning, tissues were stained for human CD31 (green) and imaged. Red present within hCD31+ structures indicated inosculation of host and implant vasculature (scale bars = 25 μm).

peptides studied. Our in vivo results showed that all gel formulations supported the formation of perfused vasculature from transplanted cells and vessel density was not attenuated in more highly crosslinked or in less degradable gels, suggesting the in vivo environment may be more permissive to vascularization. This may be of particular interest in designing therapies for clinical use, and underscores the limitations of in vitro systems to fully recapitulate the more clinically relevant in vivo environment. Overall, we have demonstrated that an injectable PEG-based synthetic material that polymerizes in situ is well suited as a vehicle for cell-based vascularization therapies and may represent a viable alternative to more invasive treatment options for ischemic diseases.

Acknowledgments: The authors gratefully acknowledge financial support for this study from the National Heart, Lung, and Blood Institute of the National Institutes of Health under award numbers R01HL085339 and R01HL118259. The authors would also like to thank Chris Strayhorn at the Histology Core at the University of Michigan School of Dentistry for assistance in generating cryosections.

Received: April 1, 2014; Revised: May 22, 2014; Published online: June 18, 2014; DOI: 10.1002/mabi.201400161

Keywords: angiogenesis; animal models; matrix metalloproteinase; mechanical properties; poly(ethylene glycol)

[1] Facts about Peripheral Artery Disease (PAD), U.S. Department of Health and Human Services, National Institutes of Health, NHLBI, NIH publication 06-5837 **2006**.
[2] R. K. Jain, P. Au, J. Tam, D. G. Duda, D. Fukumura, *Nat. Biotechnol.* **2005**, *23*, 821.
[3] X. Chen, A. S. Aledia, C. M. Ghajar, C. K. Griffith, A. J. Putnam, C. C. Hughes, J. P. George, *Tissue Eng. Part A* **2009**, *15*, 1363.
[4] X. Chen, A. S. Aledia, S. A. Popson, L. Him, C. C. Hughes, S. C. George, *Tissue Eng. Part A* **2010**, *16*, 585.
[5] P. Au, J. Tam, D. Fukumura, R. K. Jain, *Blood* **2008**, *111*, 4551.
[6] A. C. Newman, M. N. Nakatsu, W. Chou, P. D. Gershon, C. C. Hughes, *Mol. Biol. Cell* **2011**, *22*, 3791.
[7] M. N. Nakatsu, R. C. A. Sainson, J. N. Aoto, K. L. Taylor, M. Aitkenhead, S. Pérez-del-Pulgar, P. M. Carpenter, C. C. W. Hughes, *Microvasc. Res.* **2003**, *66*, 102.
[8] E. Kniazeva, A. J. Putnam, *Am. J. Physiol. Cell Physiol.* **2009**, *297*, C179.
[9] C. M. Ghajar, X. Chen, J. W. Harris, V. Suresh, C. C. Hughes, N. L. Jeon, A. J. Putnam, S. C. George, *Biophys. J.* **2008**, *94*, 1930.
[10] C. M. Ghajar, S. Kachgal, E. Kniazeva, H. Mori, S. V. Costes, S. C. George, A. J. Putnam, *Exp. Cell Res.* **2010**, *316*, 813.
[11] S. Kachgal, A. J. Putnam, *Angiogenesis* **2011**, *14*, 47.
[12] S. Kachgal, B. Carrion, I. A. Janson, A. J. Putnam, *J. Cell. Physiol.* **2012**, *227*, 3546.
[13] J. M. Melero-Martin, Z. A. Khan, A. Picard, X. Wu, S. Paruchuri, J. Bischoff, *Blood* **2007**, *109*, 4761.
[14] J. M. Melero-Martin, M. E. De Obaldia, S. Y. Kang, Z. A. Khan, L. Yuan, P. Oettgen, J. Bischoff, *Circ. Res.* **2008**, *103*, 194.
[15] K. T. Morin, R. T. Tranquillo, *Exp. Cell Res.* **2013**, *319*, 2409.
[16] P. Au, L. M. Daheron, D. G. Duda, K. S. Cohen, J. A. Tyrrell, R. M. Lanning, D. Fukumura, D. T. Scadden, R. K. Jain, *Blood* **2008**, *111*, 1302.
[17] N. Koike, D. Fukumura, O. Gralla, P. Au, J. S. Schechner, R. K. Jain, *Nature* **2004**, *428*, 138.
[18] C. Adelow, T. Segura, J. A. Hubbell, P. Frey, *Biomaterials* **2008**, *29*, 314.
[19] S. B. Anderson, C. C. Lin, D. V. Kuntzler, K. S. Anseth, *Biomaterials* **2011**, *32*, 3564.
[20] C. S. Bahney, C. W. Hsu, J. U. Yoo, J. L. West, B. Johnstone, *FASEB J.* **2011**, *25*, 1486.
[21] J. H. Collier, T. Segura, *Biomaterials* **2011**, *32*, 4198.
[22] T. P. Kraehenbuehl, L. S. Ferreira, P. Zammaretti, J. A. Hubbell, R. Langer, *Biomaterials* **2009**, *30*, 4318.

[23] M. P. Lutolf, J. L. Lauer-Fields, H. G. Schmoekel, A. T. Metters, F. E. Weber, G. B. Fields, J. A. Hubbell, *Proc. Natl. Acad. Sci. USA* **2003**, *100*, 5413.
[24] M. P. Lutolf, G. P. Raeber, A. H. Zisch, N. Tirelli, J. A. Hubbell, *Adv. Mater.* **2003**, *15*, 888.
[25] J. Patterson, J. A. Hubbell, *Biomaterials* **2010**, *31*, 7836.
[26] G. P. Raeber, M. P. Lutolf, J. A. Hubbell, *Acta Biomater.* **2007**, *3*, 615.
[27] G. P. Raeber, M. P. Lutolf, J. A. Hubbell, *Biomech. Model. Mechanobiol.* **2008**, *7*, 215.
[28] D. Seliktar, A. H. Zisch, M. P. Lutolf, J. L. Wrana, J. A. Hubbell, *J. Biomed. Mater. Res.* **2004**, *68A*, 704.
[29] S. Sokic, G. Papavasiliou, *Tissue Eng. Part A* **2012**, *18*, 2477.
[30] J. J. Moon, J. E. Saik, R. A. Poche, J. E. Leslie-Barbick, S. H. Lee, A. A. Smith, M. E. Dickinson, J. L. West, *Biomaterials* **2010**, *31*, 3840.
[31] J. E. Leslie-Barbick, C. Shen, C. Chen, J. L. West, *Tissue Eng. Part A* **2011**, *17*, 221.
[32] J. E. Leslie-Barbick, J. E. Saik, D. J. Gould, M. E. Dickinson, J. L. West, *Biomaterials* **2011**, *32*, 5782.
[33] J. S. Miller, C. J. Shen, W. R. Legant, J. D. Baranski, B. L. Blakely, C. S. Chen, *Biomaterials* **2010**, *31*, 3736.
[34] S. Sokic, G. Papavasiliou, *Acta Biomater.* **2012**, *8*, 2213.
[35] E. A. Phelps, D. M. Headen, W. R. Taylor, P. M. Thule, A. J. Garcia, *Biomaterials* **2013**, *34*, 4602.
[36] M. P. Lutolf, J. A. Hubbell, *Nat. Biotechnol.* **2005**, *23*, 47.
[37] A. H. Zisch, M. P. Lutolf, M. Ehrbar, G. P. Raeber, S. C. Rizzi, N. Davies, H. G. Schmoekel, D. Bezuidenhout, V. Djonov, P. Zilla, J. A. Hubbell, *FASEB J.* **2003**, *17*, 2260.
[38] J. E. Saik, D. J. Gould, E. M. Watkins, M. E. Dickinson, J. L. West, *Acta Biomater.* **2011**, *7*, 133.
[39] J. E. Saik, D. J. Gould, A. H. Keswani, M. E. Dickinson, J. L. West, *Biomacromolecules* **2011**, *12*, 2715.
[40] M. S. Stosich, B. Bastian, N. W. Marion, P. A. Clark, G. Reilly, J. J. Mao, *Tissue Eng.* **2007**, *13*, 2881.
[41] E. A. Phelps, N. Landazuri, P. M. Thule, W. R. Taylor, A. J. Garcia, *Proc. Natl. Acad. Sci. USA* **2010**, *107*, 3323.
[42] E. A. Phelps, K. L. Templeman, P. M. Thulé, A. J. García, *Drug Deliv. Transl. Res.* **2013**, DOI:10.1007/s13346-013-0142-2.
[43] C. M. Ghajar, K. S. Blevins, C. C. Hughes, S. C. George, A. J. Putnam, *Tissue Eng.* **2006**, *12*, 2875.
[44] M. P. Lutolf, J. A. Hubbell, *Biomacromolecules* **2003**, *4*, 713.
[45] S. Khetan, J. Burdick, *J. Vis. Exp.: JoVE* **2009**, *32*, e1590.
[46] P. J. Martens, S. H. Bryant, K. S. Anseth, *Biomacromolecules* **2003**, *4*, 283.
[47] R. K. Singh, D. Seliktar, A. J. Putnam, *Biomaterials* **2013**, *34*, 9331.
[48] S. J. Grainger, A. J. Putnam, *PLoS ONE* **2011**, *6*, 1.
[49] S. J. Grainger, B. Carrion, J. Ceccarelli, A. J. Putnam, *Tissue Eng. Part A* **2013**, *19*, 1209.
[50] M. Bracher, D. Bezuidenhout, M. P. Lutolf, T. Franz, M. Sun, P. Zilla, N. H. Davies, *Biomaterials* **2013**, *34*, 6797.
[51] B. E. Turk, L. L. Huang, E. T. Piro, L. C. Cantley, *Nat. Biotechnol.* **2001**, *19*, 661.
[52] A. W. Watkins, K. S. Anseth, *Macromolecules* **2005**, *38*, 1326.
[53] G. P. Raeber, M. P. Lutolf, J. A. Hubbell, *Biophys. J.* **2005**, *89*, 1374.
[54] C. M. Ghajar, S. C. George, A. J. Putnam, *Crit. Rev. Eukaryot. Gene Expr.* **2008**, *18*, 251.